

SDSS 0809+1729: CONNECTIONS BETWEEN EXTREMELY METAL POOR GALAXIES AND GAMMA RAY BURST HOSTS

LISA J. KEWLEY¹

University of Hawaii and
2680 Woodlawn Drive, Honolulu, HI 96822

WARREN R. BROWN², MARGARET J. GELLER, SCOTT J. KENYON, MICHAEL J. KURTZ

Smithsonian Astrophysical Observatory and
60 Garden Street MS-20, Cambridge, MA 02138

Draft version July 9, 2018

ABSTRACT

We discuss the serendipitous discovery of an extremely metal poor galaxy, SDSS 0809+1729, classified as a star in the Sloan Digital Sky Survey (SDSS). The galaxy has a redshift $z = 0.0441$ and a B -band absolute magnitude $M_B = -17.1$. With a metallicity of $\log(\text{O}/\text{H}) + 12 \sim 7.44$ or $\sim 1/20$ solar, this galaxy is among the 10 most metal poor emission-line galaxies known. SDSS 0809+1729 is a blue compact galaxy (BCG) with a stellar age of ~ 4.5 Myr, a star formation rate of $0.18 M_{\odot} \text{yr}^{-1}$, and a large gas-phase electron density ($\sim 367 \text{ cm}^{-3}$). Similar values of these parameters are common among other extremely metal poor galaxies, including I Zw 18. SDSS 0809+1729 is, however, unusual among BCGs because it lies in the same region of the luminosity-metallicity diagram as the two lowest metallicity long duration gamma ray burst (GRB) hosts. For a given B -band luminosity, both nearby GRB hosts and SDSS 0809+1729 have systematically lower metallicities than dwarf irregulars, the majority of BCGs, and normal star-forming galaxies. Because the star formation properties of SDSS 0809+1729 are similar to nearby long duration GRB hosts, SDSS 0809+1729 may be a potential GRB host. Identification of larger samples of similar extremely metal poor objects may provide important insights into the conditions required to produce long duration GRBs.

Subject headings: galaxies:starburst–galaxies:abundances–galaxies:fundamental parameters:galaxies:dwarf

1. INTRODUCTION

Extremely metal poor local galaxies are key to understanding star formation and enrichment in a nearly pristine interstellar medium (ISM). Metal poor galaxies provide important constraints on the pre-enrichment of the ISM by previous episodes of star formation. Evolutionary scenarios proposed to explain the low metallicities include metal loss from supernova-driven winds (Ferrara & Tolstoy 2000; Recchi et al. 2004), dilution of the ISM metallicity by infall of unenriched gas (Köppen & Hensler 2005), or a star formation history dominated by short bursts of star formation separated by long quiescent periods (Searle & Sargent 1972). The latter scenario is currently favored (see Kunth & Östlin 2000, for a review), but all of these mechanisms probably play some role.

Intriguingly, metal poor galaxies have recently been linked to long duration GRBs (Stanek et al. 2006; Wolf & Podsiadlowski 2006; Fruchter et al. 2006). Sollerman et al. (2005) compared the host galaxy properties of three nearby GRBs with the properties of local BCGs. They found that the luminosity and star formation rates of the GRB hosts are similar to those of local BCGs. Fruchter et al. (2006) demonstrate that long duration GRBs are concentrated in the highest surface brightness regions of their extremely blue hosts.

Stanek et al. (2006) show that five nearby GRB hosts have lower metallicities than normal star-forming galaxies of similar luminosity. Because the GRB energy released decreases steeply with increasing host metallicity, Stanek et al. propose an upper metallicity limit for cosmological GRBs of $\sim 0.15 Z_{\odot}$. Strong Lyman- α detections in GRB hosts at $z \gtrsim 2$ also support low host metallicities (Fynbo et al. 2003).

Extremely metal poor galaxies (XMPGs) are rare. Fewer than 1% of dwarf galaxies have extremely low metallicities, defined as $\log(\text{O}/\text{H}) + 12 \leq 7.65$ (Kunth & Östlin 2000; Kniazev et al. 2003). XMPGs, however, are much more common than known GRB hosts. Thus a larger sample of XMPGs is one route to understanding the environment required for the formation of the long duration GRBs. Most of the known XMPGs are gas-rich BCGs with spectra dominated by emission lines (e.g., Kunth & Sargent 1983; Thuan et al. 1995). Emission-lines provide an estimate of the gas-phase metallicity from the [O III] $\lambda 4363$ doublet. This line is particularly sensitive to the electron temperature of the gas and is strong in metal poor galaxies where H II region cooling is minimal.

Many investigators have searched for XMPGs with varying degrees of success. For more than three decades, the famous galaxy I Zw 18 was the most metal poor galaxy known, with a metallicity of $\log(\text{O}/\text{H}) + 12 \sim 7.17$ (Searle & Sargent 1972). Recently, Izotov et al. (2005) showed that the galaxy SBS 0335-052W has an even lower oxygen abundance of $\log(\text{O}/\text{H}) + 12 \sim$

Electronic address: kewley@ifa.hawaii.edu

¹ Hubble Fellow

² Clay Fellow, Harvard-Smithsonian Center for Astrophysics

7.12. Searches of SDSS spectra based on emission-lines (Izotov et al. 2004; Kniazev et al. 2003, 2004; Papaderos et al. 2006a; Izotov et al. 2006a) have uncovered few XMPGs, in agreement with previous searches of emission-line galaxies (e.g., Terlevich et al. 1991; Masegosa et al. 1994; van Zee 2000). Surveys that select on the equivalent width of strong lines such as [O II] appear to be more efficient at finding XMPGs (Ugryumov et al. 2003), but the number of known XMPGs remains small.

Here we report the serendipitous discovery of a new, very blue XMPG, SDSS 0809+1729. This galaxy is at a redshift $z = 0.0441$ and has a metallicity of $\log(\text{O}/\text{H}) + 12 \sim 7.44$. This metallicity places SDSS 0809+1729 among the 10 lowest metallicity emission-line galaxies known to date.

We describe the observations and derived quantities in § 2. We compare the properties of our galaxy with those of other XMPGs in § 3. We show that XMPGs and GRB hosts share similar spectral properties in § 4. We discuss our results and conclusions in § 5. Throughout this paper, we adopt the flat Λ -dominated cosmology as measured by the WMAP experiment ($h = 0.72$, $\Omega_m = 0.29$; Spergel et al. 2003)).

2. OBSERVATIONS AND DERIVED QUANTITIES

We discovered the low metallicity galaxy, SDSS 0809+1729, in the hypervelocity star survey of Brown et al. (2006, hereafter B06). B06 selected candidate B-stars using SDSS $(u' - g')_0$, $(g' - r')_0$, and $(r' - i')_0$ colors. SDSS 0809+1729 is classified as a star in the SDSS, but spectroscopy shows that it is a BCG with $(u' - g')_0 = 0.287$, $(g' - r')_0 = -0.416$, and $(r' - i')_0 = -0.058$ (colors have been dereddened using Schlegel et al. 1998). This dwarf galaxy is at a redshift $z = 0.0441$ and has an absolute magnitude $M_B = -17.1$. SDSS 0809+1729 has an observed $(B - R)_0 = -0.25$ and a rest frame $(B - R)_0 = -0.27$, placing it in the blue tail of a large sample of nearby BCGs (see Figure 4, Gil de Paz et al. 2003).

We observed SDSS 0809+1729 on the Blue Channel spectrograph at the 6.5m MMT telescope. In photometric conditions, we obtained a high resolution spectrum with the 832 lines mm^{-1} grating in second order, resulting in wavelength coverage of 3650Å to 4500Å at a spectral resolution of 1.2Å. In non-photometric conditions, we obtained a lower resolution spectrum with the 300 lines mm^{-1} grating, resulting in broader wavelength coverage (3400Å to 8600Å) at a resolution of 6.2 Å. Figure 1 shows both the high and low resolution spectra.

We reduced the spectra using standard IRAF³ spectral reduction tasks and flux calibrated the spectra using spectrophotometric standards. Flux calibration is accurate to $\sim 10\%$. We obtain relative flux calibration for the non-photometric low resolution spectrum. We fit the optical emission-lines with gaussians using the *splot* task in IRAF. The observed line fluxes and statistical errors are given in Table 1. For the following analysis, we corrected the emission line fluxes for reddening using the Balmer

decrement and the Cardelli et al. (1989) (CCM) reddening curve. We assumed an $R_V = A_V/E(B-V) = 3.1$ and an intrinsic $\text{H}\alpha/\text{H}\beta$ ratio of 2.85 (the Balmer decrement for case B recombination at $T = 10^4\text{K}$ and $n_e \sim 10^2 - 10^4\text{cm}^{-3}$; Osterbrock 1989).

The Balmer decrement of SDSS 0809+1729 is 2.76, consistent with zero extinction, assuming an intrinsic $\text{H}\alpha/\text{H}\beta$ ratio of 2.86 (the Balmer decrement for case B recombination at $T = 10^4\text{K}$ and $n_e \sim 10^2 - 10^4\text{cm}^{-3}$; Osterbrock 1989).

We used the [S II] $\lambda 6717$ / [S II] $\lambda 6731$ line ratio in conjunction with a 5 level model atom using the Mappings photoionization code (Sutherland & Dopita 1993) to calculate an electron density of $n_e = 367\text{cm}^{-3}$ in the S^+ zone. The [O II] $\lambda 3726$ /[O II] $\lambda 3729$ ratio gives $n_e = 195\text{cm}^{-3}$ in the O^+ zone.

We derive the gas-phase oxygen abundance following the procedure outlined in Izotov et al. (2006b). This procedure utilizes the electron-temperature (T_e) calibrations of Aller (1984) and the atomic data compiled by Stasińska (2005). Abundances are determined within the framework of the classical two-zone HII-region model (Stasińska 1980). The ratio of the auroral [O III] $\lambda 4363$ and [O III] $\lambda\lambda 4959, 5007$ emission-lines give an electron temperature in the O^{++} zone of $T_e = 19 \times 10^4\text{K}$ assuming an electron density of 195cm^{-3} . These electron temperatures are insensitive to small variations in electron density; we obtain the same T_e with an electron density of 367cm^{-3} . The electron temperature of the O^+ zone is calculated assuming $T_e(\text{O}^+) = 0.7 T_e(\text{O}^{++}) + 0.3$ (Stasińska 1980). We calculate the metallicity in the O^+ and O^{++} zones assuming

$$\text{O}/\text{H} = \text{O}^+/\text{H}^+ + \text{O}^{++}/\text{H}^+ \quad (1)$$

The resulting metallicity for SDSS 0809+1729 is $\log(\text{O}/\text{H}) + 12 \sim 7.44$. The uncertainty in the absolute O/H metallicity determination is ~ 0.1 dex. This intrinsic uncertainty is the dominant error in our metallicity determination, and includes errors in the use of simplified H II region models and possible problems with electron temperature fluctuations (Pagel & Tautvaisiene 1997). Fortunately, these errors affect all T_e -based methods in a similar way and the error in relative metallicities derived using the same method is likely to be $\ll 0.1$ dex.

We use the T_e -based metallicities to facilitate comparisons with metal poor galaxies in the literature. We also provide metallicity measurements using the theoretical strong-line diagnostics from Kewley & Dopita (2002, ; hereafter KD02), updated in Kobulnicky & Kewley (2004). The KD02 method is based on the [N II]/[O II] ratio for high metallicities ($\log(\text{O}/\text{H}) + 12 \gtrsim 8.4$), and the $([\text{O II}] + [\text{O III}])/\text{H}\beta$ (R_{23}) diagnostic for low metallicities ($\log(\text{O}/\text{H}) + 12 \lesssim 8.4$). The majority of galaxies analysed in this paper have low metallicities (as indicated by their [N II]/[O II] or [N II]/ $\text{H}\alpha$ ratios) and we use the Kobulnicky & Kewley (2004) re-calibration of the KD02 R_{23} diagnostic. The absolute error in the strong-line metallicities is ~ 0.15 dex. There is a well-known discrepancy of ~ 0.4 dex between metallicities calculated using theoretical strong-line diagnostics and diagnostics based on electron-temperature measurements. The cause of this offset is unknown (see Garnett et al. 2004b,a; Stasińska 2005, for a discussion). Until this discrepancy is resolved, absolute metallicities derived using

³ IRAF is distributed by the National Optical Astronomy Observatories, which are operated by the Association of Universities for Research in Astronomy, Inc., under cooperative agreement with the National Science Foundation.

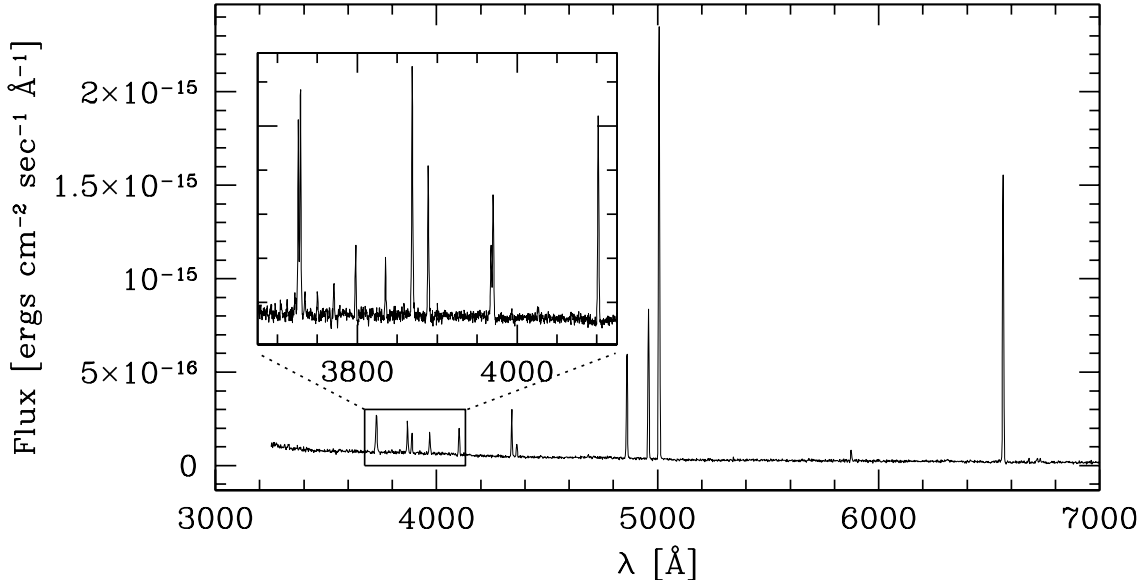


FIG. 1.— MMT spectrum of SDSS 0809+1729 obtained with the 300 lines mm^{-1} grating. SDSS 0809+1729 has a blue continuum and high $\text{H}\alpha$ and $[\text{O III}]$ equivalent widths, indicating extremely low metallicity. The inset shows the MMT spectrum obtained with the 832 line mm^{-1} grating. $[\text{O II}]$ is resolved and the higher order Balmer lines are prominent in the inset spectrum.

any method should be treated with caution. Fortunately, the difference between the strong-line and T_e diagnostics is systematic. Therefore the error in relative metallicities derived using *the same* method, regardless of the method, is $\ll 0.1$ dex (Ellison & Kewley 2005; Kewley & Ellison 2006). We therefore use metallicities based on the T_e -method, or converted into the T_e method only for relative comparisons between galaxies.

The ionization parameter of a gas q is a measure of the level of ionization that a radiation field can drive through a nebula. The ionization parameter is defined as the number of hydrogen ionizing photons passing through a unit area per second per unit hydrogen number density. We calculate the ionization parameter using the iterative prescription outlined in Kewley & Dopita (2002). The ionization parameter for SDSS 0809+1729 is $q = 1.5 \times 10^8 \text{ cm s}^{-1}$, a value that is extremely high relative to normal star-forming galaxies (e.g. Dopita et al. 2006). Such a high ionization parameter indicates that the stellar EUV radiation field and the electron temperature in SDSS 0809+1729 are stronger than in most star-forming galaxies. In Section 3 we investigate the star formation properties of SDSS 0809+1729 in more detail.

3. COMPARISON WITH OTHER EXTREMELY LOW METALLICITY GALAXIES

We compare the spectral properties of SDSS 0809+1729 with those of other XMPGs for which both (1) T_e -based metallicities are available, and (2) $\text{H}\alpha$ photometry or global spectra are available.

Because SDSS 0809+1729 is stellar in appearance, our spectra provide global estimates of galaxy properties. We note that the metallicities of the more extended low metallicity galaxies in the literature often lack global estimates of metallicity or other parameters. For example, the metallicity of 7.17 cited for J0113+0052 (Izotov et al. 2006a) was obtained from spectra of an H II region on the outskirts of the low surface brightness galaxy UGC 772.

A global metallicity estimate of UGC 772 may differ from the H II region value. Where possible, we compare the properties of SDSS 0809+1729 only with other low metallicity galaxies that have global estimates.

3.1. Stellar Population Age

The detailed star formation histories of XMPGs are difficult to measure; most XMPGs, like SDSS 0809+1729, are too far away or too compact to resolve into individual stars, even with HST. XMPGs remain a puzzle because they may be pristine galaxies undergoing their first burst of star formation or they may contain an older stellar population from previous episodes of star formation. Izotov & Thuan (1999) calculate C/O and N/O abundances for a sample of 54 BCGs. They find very little scatter in the C/O and N/O ratios in BCGs with $\log(\text{O}/\text{H}) + 12 \leq 7.6$. Izotov & Thuan suggest that such low scatter rules out time-delayed production of C and primary N and that extremely low metallicity BCGs are therefore undergoing their first burst of star formation. The fraction of neutral gas in XMPGs ($\sim 99\%$ of all baryonic mass) gives further evidence against an old stellar population (van Zee et al. 1998; Pustilnik et al. 2001). On the other hand, metal-poor galaxies may have extremely faint old stellar populations if their previous episodes of star formation occurred at very low star formation rates (Legrand et al. 2000). HST images of the nearest XMPGs provide some evidence for this picture. Color-magnitude diagrams derived from these images provide, for example, ages for I Zw 18 which range from ~ 500 Myr (Izotov & Thuan 2004) to ~ 1 Gyr (Aloisi et al. 1999); the stellar age from similar data for the metal poor BCG SBS 1415+437 is ~ 1.3 Gyr (Aloisi et al. 2005).

Although we cannot estimate the age of an old stellar population (if any) in SDSS 0809+1729, stellar population synthesis models provide an estimate of the age

of the young stellar population given a metallicity, initial mass function (IMF), and star formation history prescription. The Balmer line equivalent widths (EWs) are strongly correlated with the age of the stellar population (Schaerer & Vacca 1998; González Delgado et al. 1999). Assuming a Salpeter IMF and an instantaneous burst of star formation, the $H\beta$ equivalent width of 88.25\AA corresponds to a stellar age of ~ 4.5 Myr using the $Z = 0.001$ ($\log(O/H)+12 \sim 7.6$) models of Schaerer & Vacca (1998).

An age of 4.5 Myr corresponds to the end of the Wolf-Rayet phase for a metallicity of $Z = 0.001$. Figure 2 shows the spectrum of SDSS 0809+1729 between 4500\AA – 4800\AA with the positions of expected Wolf-Rayet features marked. The HeII $\lambda 4686$ line is clearly detected in the spectrum, but the carbon and nitrogen Wolf-Rayet features are absent. These carbon and nitrogen lines typically blend to produce the “blue bump” frequently seen in galaxies during the Wolf-Rayet phase.

The lack of prominent Wolf-Rayet features supports a stellar age of ~ 4.5 Myr. Narrow HeII emission is associated with nebular emission rather than with the broader stellar emission from Wolf-Rayet stars. It is interesting to note that our $\log(\text{HeII}/H\beta)$ ratio (-1.62) exceeds the value for pure nebular emission according to the instantaneous burst models of Schaerer & Vacca (1998). We also note that the lack of Wolf-Rayet features does not necessarily indicate that the Wolf-Rayet phase is over. Crowther & Hadfield (2006) showed that theoretical models of Wolf-Rayet stars in extremely low metallicity environments produce weaker Wolf-Rayet features by a factor of 3–6 than in galaxies at metallicities similar to the LMC.

Other XMPGs have young stellar ages similar to SDSS 0809+1729 (Table 2). All of the XMPGs in our comparison sample have stellar ages within the narrow range of 3–4.5 Myr, according to the $z = 0.001$ Schaerer & Vacca models. This age range corresponds to the middle to end of the Wolf-Rayet phase.

3.2. Star Formation Rates

The derivation of star formation rates (SFRs) for XMPGs is non-trivial. The commonly used $H\alpha$ -based SFR calibrations such as Hunter & Gallagher (1986) and Kennicutt (1998) were developed for “normal” dwarf irregular and spiral galaxies, respectively. These traditional calibrations were derived using stellar population synthesis models at solar metallicities, and are not applicable to metal-poor galaxies where the SFR can vary on short timescales. Weillbacher & Fritze-v. Alvensleben (2001) showed that (1) very low metallicity, (2) a time delay between the onset of star formation and maximum $H\alpha$ -luminosity, and (3) a varying stellar IMF yields SFRs differing by factors of 3–100 from results derived with traditional calibrations.

Bicker & Fritze-v. Alvensleben (2005, hereafter B05) use new stellar population synthesis models to calculate $H\alpha$ SFR calibrations as a function of metallicity. They show that for galaxies at low metallicities $\log(O/H)+12 \leq 8.2$ ($Z=0.004$ in B05) the constants that convert $L(H\alpha)$ into SFRs differ substantially from the solar value. B05 provide calibrations for 5 values of metallicity because they restrict the population synthesis models to the specific metallicities for which stellar evolution tracks are available. The two lowest metallicities of $Z = 0.0004$

and 0.004 correspond to $\log(O/H) + 12 = 7.23$ and 8.23 respectively. Because SDSS 0809+1729 and most of our comparison galaxies have metallicities between these values, we fit a polynomial to the inverse of the constants in B06 to obtain a calibration for arbitrary metallicity values. The $H\alpha$ calibration is then:

$$\text{SFR}(H\alpha)(M_{\odot}/\text{yr}) = 1 \times 10^{-41} (-0.0954 + 0.0644 * Z_m) L(H\alpha)(\text{ergs/s}) \quad (2)$$

where Z_m is the metallicity in units of $\log(O/H) + 12$.

Application of this calibration to the galaxies in Table 2 assumes that XMPGs have similar star formation histories. We provide two SFR estimates for each galaxy, based on either T_e -based or KD02 strong-line metallicities. The difference between the two metallicity-corrected SFR estimates is minimal for the low SFRs in XMPGs. For SDSS 0809+1729, we use $H\delta$ from our high resolution spectrum to calculate a rest-frame $H\alpha$ luminosity of 4.07×10^{40} ergs s^{-1} . If we use $H\alpha$ from our lower resolution spectrum obtained under non-photometric conditions, we obtain a similar rest-frame $H\alpha$ luminosity of 4.39×10^{40} ergs s^{-1} . Applying equation 2 gives an $\text{SFR}(H\alpha)$ of $0.18 M_{\odot}\text{yr}^{-1}$. This SFR is large compared to most of the other XMPGs; SDSS 0809+1729 has a SFR that is 10 times larger than the SFR in I Zw 18.

4. COMPARISON WITH GRB HOSTS

XMPGs can be hosts of long-duration GRBs (Stanek et al. 2006; Fruchter et al. 2006). Fruchter et al. (2006) outline some of the physics underlying the connection between long duration GRBs and their low metallicity hosts. They argue that the progenitors of the GRBs are stars massive enough to form a black hole surrounded by an accretion disk when the core collapses. Massive metal-rich stars lose mass in stellar winds and thus may not retain enough mass to collapse to black holes. Massive metal-poor stars lack the opacity to support a stellar wind. They lose little mass and, unlike their metal-rich counterparts, are not surrounded by extended HII regions. The supernova ejecta for metal-poor massive stars thus do not sweep up H and He in the surrounding wind and can produce the anomalous Type 1C supernovae associated with some nearby long duration GRBs. This plausibility argument motivates further identification and study of larger samples of XMPGs as potential long duration GRB hosts.

In this section we demonstrate that SDSS 0809+1729 has properties remarkably similar to the hosts of two of the long duration GRB hosts, GRB 030329 and GRB060218. We include a broader comparison of SDSS 0809+1729 with other XMPGs and with known long duration GRB hosts. We examine extinction, SFRs, and position with respect to luminosity-metallicity relations.

4.1. Extinction

In Table 3 we list the $H\alpha/H\beta$ ratios from the literature for the five GRB hosts in Stanek et al. (2006). The spectra of GRB hosts generally suffer very little extinction, similar to the spectra of XMPGs. We note however that a small fraction of GRB hosts are detected in the infrared and sub-mm, indicating that some GRB hosts contain dust (Frail et al. 2002; Tanvir et al. 2004; Le Floc’h et al. 2006).

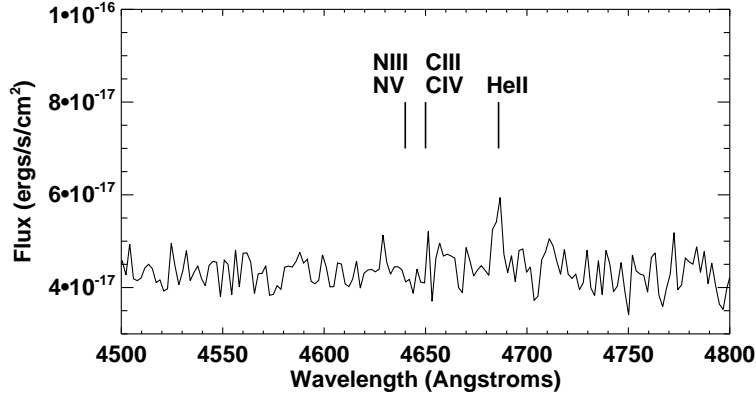


FIG. 2.— Spectrum of SDSS 0809+1729 showing the positions of expected Wolf-Rayet features. The N and C Wolf-Rayet features are undetected.

4.2. Star Formation Rates and Star Formation History

The SFRs in a few of the nearest GRB hosts have been constrained from X-ray data (Watson et al. 2004), from radio and sub-millimeter measurements (Berger et al. 2003), and from optical (Sollerman et al. 2005; Gorosabel et al. 2005), and UV observations (Fynbo et al. 2003; Christensen et al. 2004; Jakobsson et al. 2005). These studies usually yield low SFRs that span about two decades from $0.1\text{-}10 M_{\odot}\text{yr}^{-1}$.

We calculate the GRB host SFRs using the $H\alpha$ luminosity to facilitate comparisons with the $SFR(H\alpha)$ of the extremely low metallicity galaxies. The GRB hosts have low metallicities ($\log(O/H) + 12 \leq 8.0$) and therefore they are subject to the metallicity problems outlined by Weilbacher & Fritze-v. Alvensleben (2001) and B05. We therefore apply the B05 SFR calibration parameterized in equation 2, taking into account the low GRB host metallicities. The resulting SFRs are given in Table 3.

The $SFR(H\alpha)$ for GRB hosts ranges between $0.03\text{-}9 M_{\odot}\text{yr}^{-1}$. The majority (4/5) of the GRB hosts have SFRs less than $0.2 M_{\odot}\text{yr}^{-1}$. These SFRs are remarkably similar to the SFRs in the extremely low metallicity galaxies. In particular, SDSS 0809+1729 has an SFR that is very close to three of the GRB hosts ($0.18 M_{\odot}\text{yr}^{-1}$ c.f. $0.18, 0.16$, and $0.12 M_{\odot}\text{yr}^{-1}$).

Sollerman et al. (2005) found that the luminosity and SFRs of the GRB hosts are similar to those of local BCGs. Our GRB and low metallicity galaxy SFRs extend the Sollerman et al. result to lower metallicity galaxies.

For the two GRB hosts where $H\beta$ EWs are published, the age of the young stellar population is 4.5 Myr, and 9 Myr, indicating populations at the end of the Wolf-Rayet phase. Wolf-Rayet features have been detected in some extremely low metallicity galaxies (Izotov et al. 2001, 1997; Legrand et al. 1997), and have recently been detected in GRB hosts (Hammer et al. 2006). Although we do not see Wolf-Rayet features in SDSS 0809+1729, we derive a population age of 4.5 Myr and conclude that the populations is also at or near the end of the Wolf-Rayet phase.

4.3. Luminosity-Metallicity Relation

The luminosity-metallicity relation is an important tool for investigating the chemical enrichment and mass-loss in galaxies. Rubin et al. (1984) provided the first evidence that metallicity is correlated with luminosity in disk galaxies. Larger samples of nearby disk galaxies solidified the luminosity-metallicity relation (Bothun et al. 1984; Wyse & Silk 1985; Skillman et al. 1989; Vila-Costas & Edmunds 1992; Zaritsky et al. 1994; Garnett 2002; Baldry et al. 2002; Lamareille et al. 2004; Tremonti et al. 2004). A strong luminosity-metallicity relation also exists for dwarf irregular (dIrr) galaxies (Lequeux et al. 1979; Skillman et al. 1989; Richer & McCall 1995; Pilyugin 2001; Garnett 2002; Lee et al. 2004, 2006) and BCGs (Campos-Aguilar et al. 1993; Shi et al. 2005). The luminosity-metallicity relation is generally attributed to the more fundamental mass-metallicity relation that holds for star-forming disk galaxies (Tremonti et al. 2004). Low mass galaxies have larger neutral gas fractions than more massive galaxies (McGaugh & de Blok 1997; Bell & de Jong 2000; Boselli et al. 2001). Selective loss of heavy elements from low mass galaxies in supernova-driven outflows also contribute to the relation (Garnett 2002; Tremonti et al. 2004).

In Figure 3, we show where SDSS 0809+1729 (large solid circle) lies relative to the luminosity-metallicity relations of normal dIrrs (Richer & McCall 1995; Pilyugin 2001) (crosses, plusses), BCGs (Kong 2004; Shi et al. 2005), and star-forming galaxies from SDSS (Tremonti et al. 2004) (dotted line). We show the positions of the GRB hosts from Stanek et al. (2006) (squares) and the lowest metallicity galaxies from Table 2 (small filled circles). The properties of the GRB hosts are listed in Table 3. Where the $[O III] \lambda 4363$ line is available, we have recalculated the metallicities for the GRB hosts using the T_e -method. For cases where only a limited range of strong emission-lines is available, we apply the metallicity conversions of Kewley & Ellison (2006) to place the strong-line (KD02) metallicities on the same T_e -based scale. The KD02- T_e conversion is valid for KD02 metallicities $12 + \log(O/H)_{KD02} < 8.2$ and is given by:

$$12 + \log(\text{O}/\text{H})_{\text{T}_e} = \frac{(12 + \log(\text{O}/\text{H})_{\text{KD02}}) - 0.613}{0.975} \quad (3)$$

SDSS 0809+1729 lies remarkably close to the two lowest metallicity GRB hosts, GRB 060218 and GRB 030329. The XMPGs (including SDSS 0809+1729) and the GRB hosts lie offset from the dIrr and SDSS luminosity-metallicity relations; at a fixed luminosity, the XMPGs and GRB hosts are more metal poor than dIrr or SDSS galaxies. It is not clear whether this offset is a metallicity or a luminosity effect (or both). Either (1) GRB hosts and XMPGs are less enriched (by 0.2-0.4 dex) than dIrrs and SDSS galaxies for their luminosity, or (2) GRB hosts and XMPGs are over-luminous in the B -band (by 2-4 magnitudes) for their metallicities relative to dIrrs and SDSS galaxies. The B -band luminosities of nearby XMPGs include a significant contribution from emission-lines. However, the contribution of emission-lines to the total blue luminosity is 33% for SDSS 0809+1729, sufficient to raise the luminosity by only ~ 0.3 magnitudes. Stellar mass estimates derived from deep near infrared photometry may help resolve this metallicity versus luminosity issue. Nevertheless, Figure 3 indicates that studies of GRB hosts should not assume that GRB hosts lie along the normal luminosity-metallicity relation.

GRB hosts at higher redshifts also show an offset from the normal luminosity-metallicity relation; 5/7 GRB hosts at $0.4 < z < 1$ lie below the mean luminosity-metallicity relation for normal star forming galaxies at $0.4 < z < 1$ (figure 3 of Savaglio et al. 2006). The offset at $0.4 < z < 1$ between GRB hosts and normal star-forming galaxies is smaller (0.5 mag in luminosity or 0.2 dex in metallicity) than the offset apparent in Figure 3. However, this difference may result from the large errors in the metallicity estimates at $0.4 < z < 1$ (Kobulnicky & Kewley 2004).

5. CONCLUSIONS

We report the serendipitous discovery of an extremely metal poor galaxy, SDSS 0809+1729, classified as a stellar point source in the SDSS catalog. This galaxy has a metallicity of $\log(\text{O}/\text{H}) + 12 \sim 7.44$, or $\sim 1/20$ solar, placing it in the group of ten lowest metallicity emission-line galaxies. We compare the spectral properties of SDSS 0809+1729 with the spectral properties of seven known XMPGs, including I Zw 18. We apply stellar population synthesis models to derive stellar ages and we calculate SFRs, taking into account the effect of metallicity. The young stellar population in SDSS 0809+1729 has an age of ~ 4.5 Myr, corresponding to the end of the Wolf-Rayet phase. The star formation rate in SDSS 0809+1729 ($\sim 0.18 M_{\odot} \text{yr}^{-1}$) is ten times larger than the star formation rate in I Zw18.

We compare the properties of SDSS 0809+1729 and the other XMPGs with the properties of five nearby GRB hosts for which spectral data is available. We find that:

- XMPGs and GRB hosts lie in a similar region of the luminosity-metallicity diagram: both types of objects are systematically offset from the luminosity-metallicity relation defined by dIrrs, normal BCGs, and normal star-forming galaxies. For a given luminosity, XMPGs and GRB hosts are less enriched

than dIrrs, normal BCGs, and normal star-forming galaxies.

- XMPGs and GRB hosts share similar SFRs and extinction levels, strengthening the link between GRB hosts and XMPGs.
- Our new XMPG, SDSS 0809+1729, has nearly identical properties as the lowest metallicity GRB host, GRB 030329. The T_e metallicities of the two galaxies agree to within ~ 0.1 dex (the estimated error in the metallicity diagnostics is ~ 0.1 dex), and the SFRs agree to within $0.06 M_{\odot} \text{yr}^{-1}$, or 50%. While electron density measurements are unavailable for GRB hosts with luminosities similar to SDSS 0809+1729, it is interesting that the luminous host galaxy of GRB 031203 has an electron density (and stellar age) very similar to the one we measure for SDSS 0809+1729.

The similarity between XMPGs and long duration GRB hosts is remarkable. Our results suggest that SDSS 0809+1729 and other XMPGs like it are potential hosts for long duration GRBs.

Identification and analysis of larger samples of XMPGs may provide important insight into the environment where long duration GRBs occur. The serendipitous discovery of an XMPG using SDSS colors suggests that a similar color-selection method may be useful for revealing new XMPGs. Some of these objects have been missed because, like SDSS 0809+1729, they are indistinguishable from very blue stars. We will report soon on a more extensive survey to identify these objects (Brown et al. 2006, in prep.).

We thank the anonymous referee for helpful comments, and we thank M. Modjaz, K. Stanek, and D. Sanders for useful discussions. L. J. Kewley is supported by a Hubble Fellowship. W. R. Brown is supported by a Clay Fellowship. This research has made use of NASA's Astrophysics Data System Bibliographic Services. We thank the Smithsonian Institution for partial support of this research.

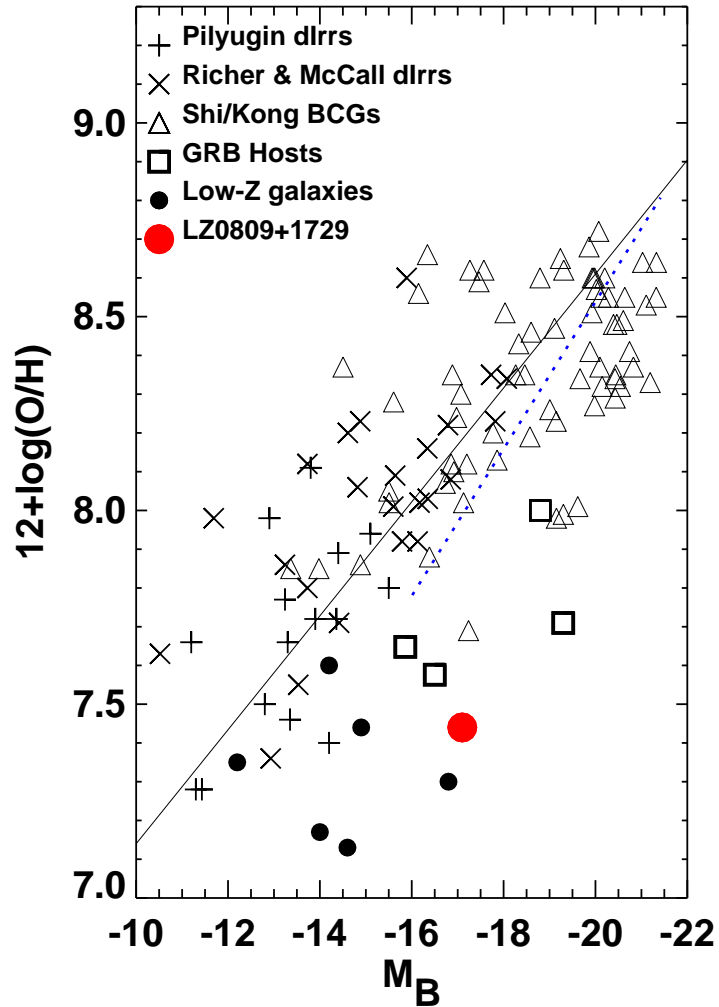


FIG. 3.— B -band absolute magnitude versus gas-phase oxygen abundance for dlrrs (crosses, Richer & McCall 1995) (Pilyugin 2001, pluses), BCGs (open triangles, Kong 2004; Shi et al. 2005), GRB hosts (open squares, Stanek et al. 2006), and extremely metal poor BCGs with T_e -based metallicities and $H\alpha$ photometry or global spectra available (solid circles). The solid line gives the mean LZ relation for dlrrs from Richer & McCall (1995) while the dotted line gives the SDSS relation for star-forming galaxies in the SDSS DR4 from Kewley & Ellison (2006, in prep). Our newly discovered XMPG, SDSS 0809+1729, is shown as a large solid red circle. SDSS 0809+1729 lies in the same region of the diagram as the two lowest metallicity GRB hosts. Note that the metallicities used in this figure, including the mean LZ relations are either (1) calculated using the T_e -method, or (2) converted into T_e metallicities using Kewley & Ellison (2006). The T_e -based metallicities are lower than strong-line metallicity estimates such as Kewley & Dopita (2002) by ~ 0.4 dex.

REFERENCES

- Aller, L. H., ed. 1984, *Physics of Thermal Gaseous Nebulae*
- Aloisi, A., Tosi, M., & Greggio, L. 1999, *AJ*, 118, 302
- Aloisi, A., van der Marel, R. P., Mack, J., Leitherer, C., Sirianni, M., & Tosi, M. 2005, *ApJ*, 631, L45
- Baldry, I. K., et al. 2002, *ApJ*, 569, 582
- Bell, E. F., & de Jong, R. S. 2000, *MNRAS*, 312, 497
- Berger, E., Cowie, L. L., Kulkarni, S. R., Frail, D. A., Aussel, H., & Barger, A. J. 2003, *ApJ*, 588, 99
- Bersier, D., et al. 2006, *ApJ*, 643, 284
- Bicker, J., & Fritze-v. Alvensleben, U. 2005, *A&A*, 443, L19
- Boselli, A., Gavazzi, G., Donas, J., & Scodreggio, M. 2001, *AJ*, 121, 753
- Bothun, G. D., Romanishin, W., Strom, S. E., & Strom, K. M. 1984, *AJ*, 89, 1300
- Brown, W. R., Geller, M. J., Kenyon, S. J., & Kurtz, M. J. 2006, *ApJ*, 647, in press Aug 10
- Campos-Aguilar, A., Moles, M., & Masegosa, J. 1993, *AJ*, 106, 1784
- Cardelli, J. A., Clayton, G. C., & Mathis, J. S. 1989, *ApJ*, 345, 245
- Christensen, L., Hjorth, J., & Gorosabel, J. 2004, *A&A*, 425, 913
- Crowther, P. A., & Hadfield, L. J. 2006, *A&A*, 449, 711
- Dopita, M. A., Fischera, J., Sutherland, R. S., Kewley, L. J., Tuffs, R. J., Popescu, C. C., van Breugel, W., Groves, B. A., & Leitherer, C. 2006, *ApJ*, 647, in press
- Ellison, S. L., & Kewley, L. J. 2005, *ArXiv Astrophysics e-prints*
- Ferrara, A., & Tolstoy, E. 2000, *MNRAS*, 313, 291
- Frail, D. A., et al. 2002, *ApJ*, 565, 829
- Fruchter, A. S., et al. 2006, *Nature*, 441, 463
- Fynbo, J. P. U., et al. 2003, *A&A*, 406, L63
- Garnett, D. R. 2002, *ApJ*, 581, 1019
- Garnett, D. R., Edmunds, M. G., Henry, R. B. C., Pagel, B. E. J., & Skillman, E. D. 2004a, *AJ*, 128, 2772
- Garnett, D. R., Kennicutt, R. C., & Bresolin, F. 2004b, *ApJ*, 607, L21
- Gil de Paz, A., Madore, B. F., & Pevunova, O. 2003, *ApJS*, 147, 29
- González Delgado, R. M., Leitherer, C., & Heckman, T. M. 1999, *ApJS*, 125, 489
- Gorosabel, J., et al. 2005, *A&A*, 444, 711
- Guseva, N. G., Papaderos, P., Izotov, Y. I., Green, R. F., Fricke, K. J., Thuan, T. X., & Noeske, K. G. 2003, *A&A*, 407, 105
- Hammer, F., Flores, H., Schaerer, D., Dessauges-Zavadsky, M., Le Floch, E., & Puech, M. 2006, *A&A*, 454, 103
- Hunt, L. K., Vanzi, L., & Thuan, T. X. 2001, *A&A*, 377, 66
- Hunter, D. A., & Elmegreen, B. G. 2004, *AJ*, 128, 2170
- Hunter, D. A., & Gallagher, III, J. S. 1986, *PASP*, 98, 5
- Izotov, Y. I., Chaffee, F. H., & Schaerer, D. 2001, *A&A*, 378, L45
- Izotov, Y. I., Lipovetsky, V. A., Chaffee, F. H., Foltz, C. B., Guseva, N. G., & Kniazev, A. Y. 1997, *ApJ*, 476, 698
- Izotov, Y. I., Papaderos, P., Guseva, N. G., Fricke, K. J., & Thuan, T. X. 2006a, *A&A*, 454, 137
- Izotov, Y. I., Stasińska, G., Guseva, N. G., & Thuan, T. X. 2004, *A&A*, 415, 87
- Izotov, Y. I., Stasińska, G., Meynet, G., Guseva, N. G., & Thuan, T. X. 2006b, *A&A*, 448, 955
- Izotov, Y. I., & Thuan, T. X. 1999, *ApJ*, 511, 639
- . 2004, *ApJ*, 616, 768
- Izotov, Y. I., Thuan, T. X., & Guseva, N. G. 2005, *ApJ*, 632, 210
- Jakobsson, P., et al. 2005, *MNRAS*, 362, 245
- Kennicutt, R. C. 1998, *ARA&A*, 36, 189
- Kewley, L. J., & Dopita, M. A. 2002, *ApJS*, 142, 35
- Kewley, L. J., & Ellison, S. 2006, in preparation
- Kniazev, A. Y., Grebel, E. K., Hao, L., Strauss, M. A., Brinkmann, J., & Fukugita, M. 2003, *ApJ*, 593, L73
- Kniazev, A. Y., Pustilnik, S. A., Grebel, E. K., Lee, H., & Pramskij, A. G. 2004, *ApJS*, 153, 429
- Kniazev, A. Y., Pustilnik, S. A., Masegosa, J., Márquez, I., Ugryumov, A. V., Martin, J.-M., Izotov, Y. I., Engels, D., Brosch, N., Hopp, U., Merlino, S., & Lipovetsky, V. A. 2000, *A&A*, 357, 101
- Kobulnicky, H. A., & Kewley, L. J. 2004, *ApJ*, 617, 240
- Kong, X. 2004, *A&A*, 425, 417
- Kong, X., Cheng, F. Z., Weiss, A., & Charlot, S. 2002, *A&A*, 396, 503
- Köppen, J., & Hensler, G. 2005, *A&A*, 434, 531
- Kunth, D., & Östlin, G. 2000, *A&A Rev.*, 10, 1
- Kunth, D., & Sargent, W. L. W. 1983, *ApJ*, 273, 81
- Lamareille, F., Mouhcine, M., Contini, T., Lewis, I., & Maddox, S. 2004, *MNRAS*, 350, 396
- Le Floch, E., Charmandaris, V., Forrest, W. J., Mirabel, I. F., Armus, L., & Devost, D. 2006, *ApJ*, 642, 636
- Lee, H., Skillman, E. D., Cannon, J. M., Jackson, D. C., Gehrz, R. D., Polomski, E. F., & Woodward, C. E. 2006, *ApJ*, preprint astro
- Lee, J. C., Salzer, J. J., & Melbourne, J. 2004, *ApJ*, 616, 752
- Legrand, F., Kunth, D., Roy, J.-R., Mas-Hesse, J. M., & Walsh, J. R. 1997, *A&A*, 326, L17
- . 2000, *A&A*, 355, 891
- Lequeux, J., Peimbert, M., Rayo, J. F., Serrano, A., & Torres-Peimbert, S. 1979, *A&A*, 80, 155
- Masegosa, J., Moles, M., & Campos-Aguilar, A. 1994, *ApJ*, 420, 576
- McGaugh, S. S., & de Blok, W. J. G. 1997, *ApJ*, 481, 689
- Melnick, J., Heydari-Malayeri, M., & Leisy, P. 1992, *A&A*, 253, 16
- Modjaz, M., et al. 2006, *ApJ*, 645, L21
- Osterbrock, D. E. 1989, *Astrophysics of gaseous nebulae and active galactic nuclei* (University Science Books)
- Pagel, B. E. J., & Tautvaisiene, G. 1997, *MNRAS*, 288, 108
- Papaderos, P., Guseva, N. G., Izotov, Y. I., Noeske, K. G., Thuan, T. X., & Fricke, K. J. 2006a, *ArXiv Astrophysics e-prints*
- Papaderos, P., Izotov, Y. I., Guseva, N. G., Thuan, T. X., & Fricke, K. J. 2006b, *A&A*, preprint astro
- Pilyugin, L. S. 2001, *A&A*, 374, 412
- Prochaska, J. X., Bloom, J. S., Chen, H.-W., Hurley, K. C., Melbourne, J., Dressler, A., Graham, J. R., Osip, D. J., & Vacca, W. D. 2004, *ApJ*, 611, 200
- Pustilnik, S., Kniazev, A., Pramskij, A., Izotov, Y., Foltz, C., Brosch, N., Martin, J.-M., & Ugryumov, A. 2004, *A&A*, 419, 469
- Pustilnik, S. A., Brinks, E., Thuan, T. X., Lipovetsky, V. A., & Izotov, Y. I. 2001, *AJ*, 121, 1413
- Pustilnik, S. A., Engels, D., Kniazev, A. Y., Pramskij, A. G., Ugryumov, A. V., & Hagen, H.-J. 2006, *Astronomy Letters*, 32, 228
- Recchi, S., Matteucci, F., D'Ercole, A., & Tosi, M. 2004, *A&A*, 426, 37
- Richer, M. G., & McCall, M. L. 1995, *ApJ*, 445, 642
- Rubin, V. C., Ford, W. K., & Whitmore, B. C. 1984, *ApJ*, 281, L21
- Savaglio, S., Glazebrook, K., & Le Borgne, D. 2006, in *American Institute of Physics Conference Series*, ed. S. S. Holt, N. Gehrels, & J. A. Nousek, 540–545
- Schaerer, D., & Vacca, W. D. 1998, *ApJ*, 497, 618
- Schlegel, D. J., Finkbeiner, D. P., & Davis, M. 1998, *ApJ*, 500, 525
- Searle, L., & Sargent, W. L. W. 1972, *ApJ*, 173, 25
- Shi, F., Kong, X., Li, C., & Cheng, F. Z. 2005, *A&A*, 437, 849
- Skillman, E. D., Kennicutt, R. C., & Hodge, P. W. 1989, *ApJ*, 347, 875
- Sollerman, J., Östlin, G., Fynbo, J. P. U., Hjorth, J., Fruchter, A., & Pedersen, K. 2005, *New Astronomy*, 11, 103
- Spergel, D. N., et al. 2003, *ApJS*, 148, 175
- Stanek, K. Z., et al. 2006, *ApJ*, preprint astro
- Stasińska, G. 2005, *A&A*, 434, 507
- Stasińska, G. 1980, *A&A*, 84, 320
- Sutherland, R. S., & Dopita, M. A. 1993, *ApJS*, 88, 253
- Tanvir, N. R., et al. 2004, *MNRAS*, 352, 1073
- Terlevich, R., Melnick, J., Masegosa, J., Moles, M., & Copetti, M. V. F. 1991, *A&AS*, 91, 285
- Thuan, T. X., Izotov, Y. I., & Lipovetsky, V. A. 1995, *ApJ*, 445, 108
- Tremonti, C. A., et al. 2004, *ApJ*, 613, 898
- Ugryumov, A. V., Engels, D., Pustilnik, S. A., Kniazev, A. Y., Pramskij, A. G., & Hagen, H.-J. 2003, *A&A*, 397, 463
- van Zee, L. 2000, *ApJ*, 543, L31
- van Zee, L., Westpfahl, D., Haynes, M. P., & Salzer, J. J. 1998, *AJ*, 115, 1000
- Vila-Costas, M. B., & Edmunds, M. G. 1992, *MNRAS*, 259, 121

- Watson, D., Hjorth, J., Jakobsson, P., Pedersen, K., Patel, S., & Kouveliotou, C. 2004, *A&A*, 425, L33
- Weilbacher, P. M., & Fritze-v. Alvensleben, U. 2001, *A&A*, 373, L9
- Wolf, C., & Podsiadlowski, P. 2006, *MNRAS*, preprint astro
- Wyse, R. F. G., & Silk, J. 1985, *ApJ*, 296, L1
- Zaritsky, D., Kennicutt, R. C., & Huchra, J. P. 1994, *ApJ*, 420, 87

TABLE 1
 LINE INTENSITIES FOR SDSS
 0809+1729

λ_0 Ion (\AA)	$F(\lambda)/F(\text{H}\beta)^a$
3726 [OII]	0.20 ± 0.02
3729 [OII]	0.25 ± 0.02
3750 H12	0.022 ± 0.006
3771 H11	0.033 ± 0.005
3798 H10	0.066 ± 0.009
3835 H9	0.055 ± 0.008
3869 [NeIII]	0.29 ± 0.02
3889 H8+HeI	0.17 ± 0.01
3967 [NeIII]	0.079 ± 0.007
3970 H7	0.138 ± 0.009
4026 HeI	0.013 ± 0.003
4101 H δ	0.24 ± 0.01
4340 H γ	0.415 ± 0.009
4363 [OIII]	0.129 ± 0.006
4686 HeII	0.024 ± 0.006
4681 H β	1.00 ± 0.01
4959 [OIII]	1.37 ± 0.02
5007 [OIII]	4.03 ± 0.04
5876 HeI	0.105 ± 0.007
6563 H α	2.76 ± 0.03
6678 HeI	0.034 ± 0.006
6717 [SII]	0.042 ± 0.007
6731 [SII]	0.038 ± 0.007
7065 HeI	0.035 ± 0.006
7136 [ArIII]	0.025 ± 0.07
F(H β) ^b	33.0 ± 3.3
EW(H β)	88.3 ± 0.8
-	-

^aErrors in fluxes relative to H β include poisson statistical errors for both F(λ) and F(H β)

^bF(H β) in units of 1×10^{-16} ergs/s/cm². Error includes both statistical errors and 10% error in the absolute flux calibration.

TABLE 2
COMPARISON BETWEEN SPECTRAL PROPERTIES OF EXTREMELY LOW METALLICITY GALAXIES

ID	Hubble Type	v (km s ⁻¹)	log(O/H)+12		M_B	EW(H β)	Stellar Age (Myr)	L(H α) (ergs s ⁻¹)	SFR (M $_{\odot}$ /yr)		N_e (SII) (cm ⁻²)	H α /H β
			T _e	KD02					T _e	KD02		
SBS0335-052W ^a	dIrr,BCG	4017	7.13	7.5	-14.6	109	4	5.92×10^{39} g	0.021	0.022	330	2.74
I Zw 18 ^b	BCG	751	7.17	7.6	-14.0	104.5	4	4.92×10^{39} g	0.018	0.019	104.7	2.89
SBS0335-052E ^c	BCG	4057	7.30	7.5	-16.8	89-382	3-4.5	1.35×10^{41} g	0.51	0.53		2.74
HS0822+3542 ^c	BCG	732	7.35	7.6	-12.2	292	3	9.82×10^{38} g	0.004	0.004	...	2.74
HS2134+0400 ^d	BCG	5070	7.44	7.8	-14.9	214	3	8.29×10^{39} g	0.031	0.033	236	3.00
SDSS 0809+1729	BCG	13232	7.44	7.8	-17.1	88.3	4.5	4.64×10^{40}	0.18	0.19	367	2.76
SBS 1415+437 ^f	BCG	609	7.60	7.9	-14.2	134,166	4	4.59×10^{39} g	0.018	0.019	60,90	2.71,2.81

^aReferences for data:Pustilnik et al. (2004); Izotov et al. (2005); Papaderos et al. (2006b)

^bReference for data:Kong et al. (2002); Gil de Paz et al. (2003)

^cReferences for data:Melnick et al. (1992); Hunt et al. (2001); Izotov et al. (2001); Pustilnik et al. (2004); Papaderos et al. (2006b)

^dReferences for data:Pustilnik et al. (2006); Gil de Paz et al. (2003); H α is not a global measurement

^eReferences for data:Kniazev et al. (2000); Gil de Paz et al. (2003); Hunter & Elmegreen (2004)

^fReferences for data:Gil de Paz et al. (2003); Guseva et al. (2003)

^gWe calculated L(H α) using the observed H α fluxes from references (a-f); L(H α) has been converted to rest-frame and corrected L(H α) for extinction using the Balmer Decrement and the Cardelli et al. (1989) reddening curve.

TABLE 3
COMPARISON BETWEEN SPECTRAL PROPERTIES OF GRB HOSTS AND SDSS 0809+1729

ID	v (km s ⁻¹)	log(O/H)+12		M_B	EW(H β)	Stellar Age (Myr)	L(H α) (ergs s ⁻¹)	SFR (M_\odot)		N_e (SII) (cm ⁻²)	H α /H β
		T_e	KD02					T_e	KD02		
GRB 980425 ^a	2549	...	8.5	-17.65	4.14×10^{40h}	0.18	0.19	...	2.45
GRB 031203 ^b	31629	7.8 ^g	8.1	-19.3	90.72	4.5	2.17×10^{42h}	8.81	9.23	300	8.94
GRB 020903 ^c	74950	8.0 ^f	8.3	-18.8	36.08	9	3.76×10^{40i}	0.16	0.16	...	3.26
GRB 060218 ^d	10046	7.6 ^g	8.1	-15.86	8.17×10^{39h}	0.03	0.03	...	3.0
GRB 030329 ^e	50516	7.5 ^g	8.0	-16.5	3.00×10^{40h}	0.12	0.13	...	2.77
SDSS 0809+1729	13232	7.44	7.8	-17.1	88.3	4.5	4.64×10^{40}	0.18	0.19	367	2.76

^aReferences for data:Sollerman et al. (2005); Stanek et al. (2006)

^bReference for data:Prochaska et al. (2004); Sollerman et al. (2005); Stanek et al. (2006)

^cReferences for data:Stanek et al. (2006); Bersier et al. (2006); Hammer et al. (2006)

^dReferences for data:Stanek et al. (2006); Modjaz et al. (2006)

^eReferences for data:Gorosabel et al. (2005); Sollerman et al. (2005); Stanek et al. (2006)

^fMetallicity is calculated using the T_e method and the [OIII] 4363 line in Hammer et al. (2006)

^g T_e metallicity is calculated using the KD02- T_e conversion from Kewley & Ellison (2006) (equation 3)

^hWe calculated L(H α) using the observed H α fluxes from references (a-f); L(H α) has been converted to rest-frame and corrected L(H α) for extinction using the Balmer Decrement and the Cardelli et al. (1989) reddening curve.